Synthesized carbon structure from local fruit using rapid thermal annealing process

Anisse Chiali[1, 2, *], Fayçal Dergal[4], Meymoun Bellaoui[2], Lamine Nait Bouda[3], Djamila Atmani[3], Nasr Eddine Chabane Sari[2], Nassera Ghellai[2], Noureddine Choukchou-Braham[4, 5]

[1] École Supérieure en sciences appliquées de Tlemcen, ESSA-Tlemcen, 13000 - Algérie

[2] Unité matériaux et énergies renouvelables (URMER), University of Tlemcen, Algeria

[3] The Center for the Development of Advanced Technologies (CDTA) 16000, Algiers

[4] Centre de Recherche Scientifique et Technique en Analyses Physico - Chimiques (C.R.A.P.C). 42004, Tipaza Algeria

[5] Laboratoire de Catalyse et Synthèse en Chimie Organique. Département de Chimie, Faculté des Sciences. Université A. Belkaid – Tlemcen, B.P. 119 Tlemcen, Algérie

** Correspondence: a.chiali.essat@gmail.com; Tel.: +213 (0) 557 866 231*

Abstract

Structural and chemical characteristics of easily made graphite foam synthesized from the Arbutus Unedo fruit with rapid thermal process and have been studied using XRD, scanning electron microscopy and Raman micro spectroscopy. Chemically, the carbon atoms in these materials are found to have identical bonding states akin to those with pure graphite single crystals [1].

Herein a rapid thermal annealing (RTA) strategy is proposed to mass produce a mesoporous carbon structures (600 °C). Microstructural studies indicate that they have a similar cellular morphology, with the cell walls comprising carbon layers. The walls can be smooth or stepped depending upon the orientation of carbon layers with respect to the cells. The ligaments between the neighboring cells and the junctions of ligaments (corners of three or more cells) distinctly show layers of carbon planes, irregular flakes, and beam-like protruding structures made up of folded layers of graphite [2].

Keywords: porous carbon foam, carbon structure, acid dehydration, XRD, Raman spectroscopy, rapid thermal annealing.

1. Introduction

Biomass or bio waste derived from agricultural plants or forest residues, and marine, industrial or home wastes, are economical, renewable, and widely current all over the world. In latest decades, they are increasingly used as sources to enhance functional carbon materials. In addition, many natural biomass materials include heteroatoms like N, which can be in part retained in the resulting carbon, supporting to improve the electrical conductivity or catalytic activity. [1, 33]

Carbonaceous materials have been confirmed to be produced from a large range of biomass materials which include lignin,[34] corncob [35], ginkgo leaves,[36] cornstalk, [37] bacterial cellulose, banana peel, [38] peanut shells,[39] willow catkins, [40] [41] pinecone hull, bamboo chopsticks, [42] Camellia japonica, [43] pine core shells, [44] and so forth. As most biomass sources are insoluble, they are commonly hard to be assembled in the templating routes; however, there still exist some examples realizing the conversion of the insoluble biomass into porous carbon substances through soft or hard-templating methods [45]. In addition, some biomass composed of hemicellulose, cellulose, sugar or lignin can be partly transformed into soluble organic compounds, which are then prepared to be used in templating routes. For instance, [46, 35, 47].

The soluble hemicelluloses hydrolysis products of spruce or corncob have been utilized together with silica nanoparticles to prepare hollow carbon spheres. [48] Also, sugar containing juices have been extracted from biomass materials like sugar cane, potato, watermelon and grape, which should be transformed into stable carbon sphere, hole carbon sphere, hole carbon bowl or hole multihole carbon bowl through using hydrothermal treatment and soft- templating method. [49]. Due to its elevate thermal conductivity, low density, and large specific surface area, carbon structure is identified as a suitable material for thermal administration [50, 51]. It is chiefly focused on electronic energy warmth sinks [52]. Many works have been carried out to better apprehend carbon shape heat transfer phenomena.

Till today, for an industrial solution, heat exchangers based totally on aluminum and copper are the most frequent thermal materials. Thus, countless issues restrict the development of carbon structure warmth exchangers, stopping them from being without problems on hand in the market.

2. Materials and Methods

Arbutus Unedo Strawberry from Ain Fezza, Tlemcen, Algeria. Concentrated sulfuric acid (96%, Sigma Aldrich). D.I. water from URMER facilities. SEM JEOL JSM 6360.

LabRAM HR Evolution system (Horiba Jobin-Yvon) at CDTA (The Center for the Development of Advanced Technologies, Algiers.

2.1. Sucrose Extraction from (Arbutus Unedo L.) Strawberry

Strawberry fruits (Arbutus Unedo L.) were harvested near Ain Fezza in Tlemcen, Algeria in November 2017. Approximately 6 kg of fruits of uniform ripeness

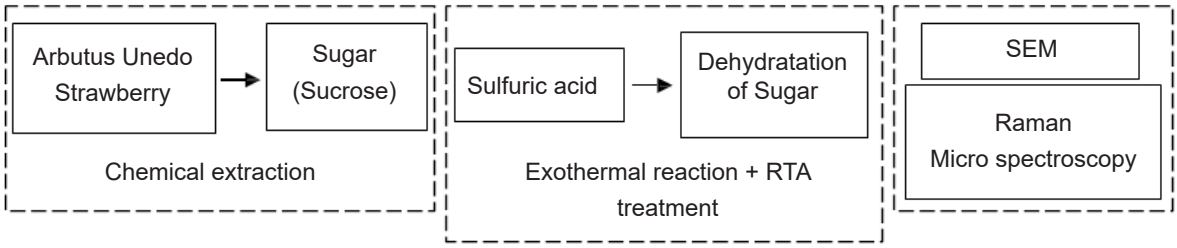

Scheme 1. The flow chart for the experiment (extraction, reaction, and characterization).

(red color) were used for the experiment.

According to [8], sucrose, glucose, sucrose, and maltose were the soluble sugars identified and quantified in the amount of 27.8, 21.5, 1.8, and 1.11% dry weight, respectively.

The (Arbutus Unedo L.) strawberry was cut into pieces with a volume of about 1 cm3. The pieces were washed with acetone and immersed in DI water for 30 minutes. After rinsing several times, the samples (about 3 g) were crushed in a mortar until no obvious chunks were visible.

Then, we macerated the plant material to make pulp, finely mincing it with a knife, and grating and processing in a blender.

We poured the pulp into a glass container. Then we added an equal amount of DI water to the container. We stirred the pulp and water for 30 minutes.

We lined a different glass container with a paper filter and placed the mixture in the filter. Then we filtered the juice into the second container. We scraped the pulp from the filter and mixed it with more warm DI water, as we did previously. Then we filtered the resulting juice in the same manner using a new paper filter. We repeated the process of extracting the juice from the pulp at least three more times.

We put the juice in a pot on a stove and turned the stove burner on low-medium heat, bringing the juice to a simmer. We then heated the juice for several minutes until its water portion cooked off and syrup developed.

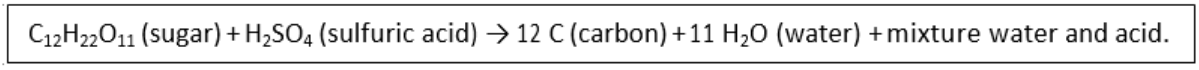

Figure 2. Chemical reaction between sucrose and sulfuric acid.

Sucrose is a carbohydrate, so when we remove the water from the molecule, we will basically leave with elemental carbon. The dehydration reaction is a type of elimination reaction.

Although the sugar is dehydrated, the water isn't 'lost' in the reaction. Some of it remains as a liquid in the acid. Since the reaction is exothermic, much of the water is boiled off as steam.

A typical reaction is as follows: 5 ml of concentrated sulfuric acid was added to a 20 ml glass scintillation vial containing 1 g of sucrose. The mixture was stirred briefly, then placed on a 200°C hotplate and stirred vigorously. During this period, the colorless mixture first turned yellow, then a deep red-brown, and finally brown and black, coating the walls of the flask with an opaque film, a transformation that took roughly two minutes. The product was an opaque black porous material [9]. As final step, long thermal annealing is not recommended here because the carbons of the graphene fakes can rapidly decompose in air at high temperatures. After rapid thermal annealing (600 °C during 10 min), the resulting material was removed from the furnace and cooled down to room temperature naturally. After thermal annealing, the product was an opaque black porous material, and dehydrated. It has collected and stored as a powder.

2.2 Characterization Methods

The surface morphologies of the samples were examined by scanning electron microscopy (SEM jeol JSM 6360).

3. Results and discussion

3.1 Microstructural Features Observed in the SEM

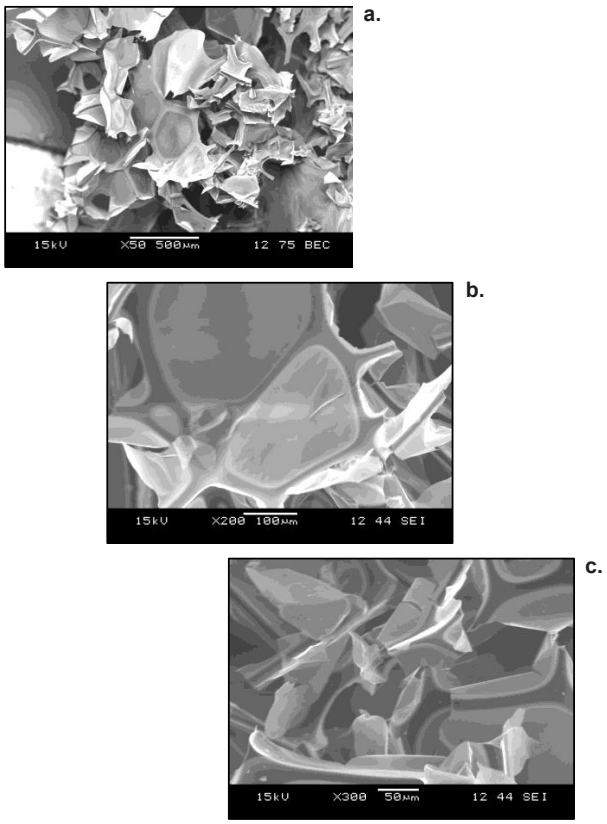

Figure 3. SEM pictures with different zoom (500µm, 100µm and 50µm) of the cellular structure of the graphite foam obtained.

Raman spectra were obtained on an HR Evolution (HORIBA JOBIN YVON) with 532 nm laser. XRD characterization was obtained on Figure 3 shows the microstructure of graphitized foam taken with SEM. Some observations can be made directly from this image. It is clear that these foams are not reticulated networks of linear rods as seen in typical glassy carbon foams [10]. They are similar to the structures reported by Klett et al. At Oak Ridge, they exhibited a cellular morphology in which the cell walls were made up of layers of carbon material. Cell diameters vary, mostly in the vicinity between 60 to 100 mm. The cell structure of these graphitized samples is significantly less smooth and less uniform than that of foam that has been carbonized but not graphitized.

The cell walls have an open, interconnected pore structure. Pores in the graphitized sample appear to be larger and the majority of the pore openings have irregular ruptured edges and sharp corners, indicating brittle fracture during formation. Figure 3 shows a close-up view of such pores (figures 3a,

3.b and 3.c). The morphology of these openings, especially the sharpness of the cracks, is expected to be important for the failure mechanisms of these structures [11]. It may be worth investigating how the shape and crack sizes of pore openings depend upon various parameters such as variation of temperature and sulfuric acid concentration with time.

3.2 Microstructural Features Analyzed by Raman Micro Spectroscopy

The heat transfer in solids is mainly governed by the properties of photon propagation. Therefore, the use of Raman spectroscopy should be great for the characterization of the carbon foams. The unique Raman spectra of graphite normally consist of mainly three strong features [12].

Raman spectroscopy was used to evaluate the chemical functionalization of the carbon foam (Figure 5).

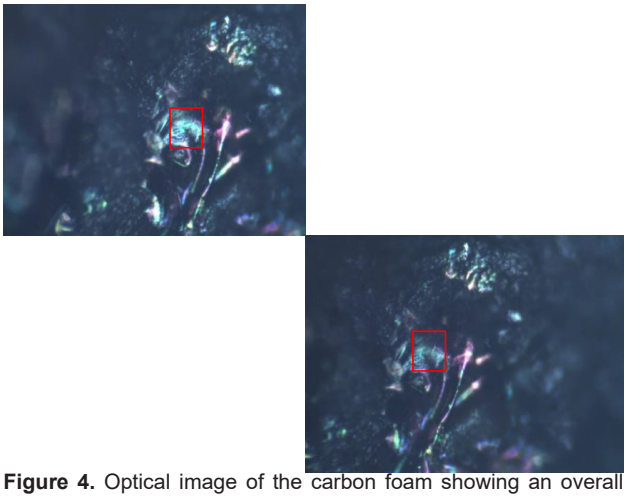

Figure 4. Optical image of the carbon foam showing an overall view of the porous structure of the foam. The squares show the areas of the carbon foam where the Raman spectra were obtained.

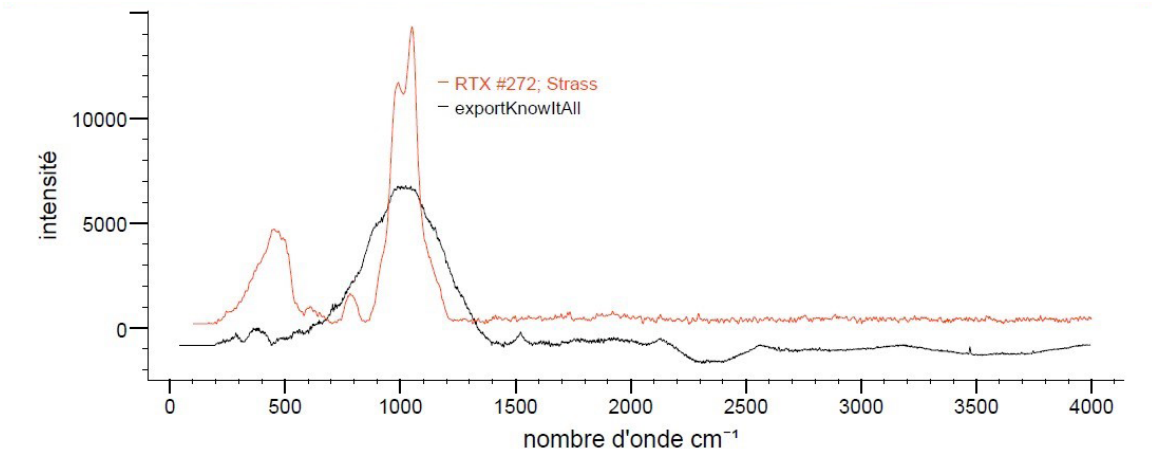

Figure 5. Raman spectrum of dark area in optical image with the signature of amorphous carbon residue. According the Raman database, the carbon structure obtained looks like strass carbon.

The Raman spectrum (Fig. 5.) of the structure showed a broad background with a weak broad peak at 1000 cm−1 and a shoulder at 1500 cm−1. The peak at 1500 cm−1 indicated the presence of sp2 polyaromatic carbon networks, whereas the origin of the peak at 1500 cm−1 is hypothesized to be trans-polyacetylene like chains at grain boundaries.

This peak also appears in the Raman spectra of nanodiamonds with significant disorder [13]. The Raman spectrum strongly resembles that of other disordered pyrolytic carbons [14, 15] and differs substantially from multilayer graphene, which shows a much more ordered structure [16].

We noted in the introduction that the acid-mediated dehydration of sugar has a long history, both as a classroom demonstration and as an object of intensive scientific study. The reaction mechanism is complex, but we speculated that it begins with elimination and rearrangement reactions through a hydroxymethylfurfural pathway [17]. The sulfuric acid removes H2O units from the sugar, resulting in extensively sp2 bonded molecular precursors such as hydroxymethylfurfural. These precursors then most likely dehydratively polymerize and coalesce into larger polyaromatic species.

This sequence of events is reflected in our observations, in particular, the Raman spectrum of the unannealed films. For shorter dehydration times, the Raman spectra are essentially featureless with a broad high background. For longer dehydration times,

the Raman spectra are essentially featureless with a broad high background. For longer dehydration times, the peak begins to develop along with a shoulder at 1500 cm−1 that is attributed to the development of conjugated polyacetylene chains.

In this model, small (~50 nm) domains of carbon carbon are randomly oriented and are weakly linked by non-carbon carbon chains. Indeed, while graphitizing, carbons tend to be quite soft; our carbons were hard and brittle, which can be easily seen when scraping the film with a set of forceps. This brittleness is attributable to the strong cross- linking and random orientations of nanocrystalline graphite.

4. Conclusions

We have presented a structural study of carbon carbon structure rapidly with thermal process and based on a simple acid dehydration of sucrose. The precursor was extracted from a common fruit in Tlemcen: Arbutus Unedo L. In addition, their chemical material (carbon structure) can be tuned by choosing different starting carbohydrates (fructose, glucose).

Acknowledgments

Anisse Chiali thanks Prof. N.E. Chabane-Sari and Prof. N. Ghellai for their support and advice and Prof. Ghouti Merad, Director of CDTA – Algiers for his continued support and invaluable help. I thank Dr. Nait Bouda Lamine for the SEM and Raman Spectroscopy characterizations as well as Dr. Athmani Djamila for the XRD characterizations.

References

[1] Papaioannou, N., Marinovic, A., Yoshizawa, N., Goode, A. E., Fay, M., Khlobystov, A. & Sapelkin, A. (2018). Structure and solvents effects on the optical properties of sugar-derived carbon nanodots. Scientific reports, 8(1), 1-10.

[2] Ding, C., Wu, S., Zhang, Y., Wu, Y., Geng, X., Huang, X., ... & Wang, A. (2021). Sugar blower protocol enabling superior electromagnetic wave absorption of porous micro pipeline carbon materials. Journal of Materials Chemistry A, 9(30), 16395-16404.

[3] Liu, X., Wu, Y., Ye, H., Chen, J., Xiao, W., Zhou, W., ... & Yuan, Z. (2021). Modification of sugar- based carbon using lanthanum and cobalt bimetal species for effective adsorption of methyl orange. Environmental Technology & Innovation, 23, 101769.

[4] Vannarath, A., & Thalla, A. K. (2021). Synthesis and characterisation of an ultra-light, hydrophobic and flame-retardant robust lignin-carbon foam for oil-water separation. Journal of Cleaner Production, 325, 129263.

[5] Ye, X., Wang, H., Chen, Z., Li, M., Wang, T., Wu, C., ... & Shen, Z. X. (2021). Maximized pseudo- graphitic content in self-supported hollow interconnected carbon foam boosting ultrastable Na-ion storage. Electrochimica Acta, 371, 137776.

[6] Guo, Z., Long, B., Gao, S., Luo, J., Wang, L., Huang, X., ... & Gao, J. (2021). Carbon nanofiber based superhydrophobic foam composite for high performance oil/water separation. Journal of Hazardous Materials, 402, 123838.

[7] Bois, R., Pezron, I., Rotureau, P., Van Hecke, E., Fayet, G., & Nesterenko, A. (2021). Foaming behavior of sugar-based surfactants: influence of molecular structure and anticipation from surface properties. Journal of Dispersion Science and Technology, 1-12.

[8] Rodríguez, E., Diez, M. A., Antuña-Nieto, C., López-Antón, M. A., García, R., & Martínez- Tarazona, M. R. (2021). An insight into the role of biomass, biocompounds and synthetic polymers as additives to coal for the synthesis of carbon foams. Journal of Analytical and Applied Pyrolysis, 160, 105359.

[9] Wang, J., Chaemchuen, S., Chen, C., Heynderickx, P. M., Roy, S., & Verpoort, F. (2022). N- functionalized hierarchical carbon composite derived from ZIF-67 and carbon foam for efficient overall water splitting. Journal of Industrial and Engineering Chemistry, 105, 222-230.

[10] Mäkelä, E. (2021). Hydrotreatment of lignocellulose-derived molecules to renewable fuels and chemicals.

[11] Ganiyu, S. O., de Araújo, M. J. G., de Araujo Costa, E. C., Santos, J. E. L., dos Santos, E. V., Martinez-Huitle, C. A., & Pergher, S. B. C. (2021). Design of highly efficient porous carbon foam cathode for electro-Fenton degradation of antimicrobial sulfanilamide. Applied Catalysis B: Environmental, 283, 119652.

[12] N. N. Wang, Y. X. Wang, X. Xu, T. Liao, Y. Du, Z. C. Bai, S. X. Dou, ACS Appl. Mater. Interfaces 2018, 10, 9353.

[13] Wu, S., Chen, D., Zhao, G., Cheng, Y., Sun, B., Yan, X., ... & Zhang, X. (2022). Controllable synthesis of a robust sucrose-derived bio-carbon foam with 3D hierarchical porous structure for thermal insulation, flame retardancy and oil absorption. Chemical Engineering Journal, 134514.

[14] Singh, S., Chaudhary, P., Srivastava, R., Tripathi, R. K., Kumar, R., & Yadav, B. C. (2021). Improved growth of nano tin ferrites with their decoration on carbon foam for wastewater treatment. Environmental Nanotechnology, Monitoring & Management, 16, 100546.

[15] Ye, X., Wang, H., Chen, Z., Li, M., Wang, T., Wu, C., ... & Shen, Z. X. (2021). Maximized pseudo - graphitic content in self-supported hollow interconnected carbon foam boosting ultrastable Na-ion storage. Electrochimica Acta, 371, 137776.

[16] a) J. Hayashi, A. Kazehaya, K. Muroyama, A. P. Watkinson, Carbon 2000, 38, 1873; b) S. Ucar, M. Erdem, T. Tay, S. Karagoz, Clean Technol. Environ. Policy 2015, 17, 747; c) L. M. Yue, Q. Z. Xia, L. W. Wang, L. L. Wang, H. DaCosta, J. Yang, X. Hu, J. Colloid Interface Sci. 2018, 511, 259.

[17] Wu, S., Chen, D., Zhao, G., Cheng, Y., Sun, B., Yan, X., ... & Zhang, X. (2022). Controllable synthesis of a robust sucrose-derived bio-carbon foam with 3D hierarchical porous structure for thermal insulation, flame retardancy and oil absorption. Chemical Engineering Journal, 134514.

[18] a) Y. Li, S. Xu, X. Wu, J. Yu, Y. Wang, Y.-S. Hu, H. Li, L. Chen, X. Huang, J. Mater. Chem. A 2015, 3, 71; b) L. Jiang, L. Sheng, Z. Fan, Sci. China Mater. 2018, 61, 133.

[19] Wang, P., Zhang, G., Li, M. Y., Yin, Y. X., Li, J. Y., Li, G., ... & Guo, Y. G. (2019). Porous carbon for high-energy density symmetrical supercapacitor and lithium-ion hybrid electrochemical capacitors. Chemical Engineering Journal, 375, 122020.

[20] Oyedotun, K. O., Barzegar, F., Mirghni, A. A., Khaleed, A. A., Masikhwa, T. M., & Manyala, N. (2018). Examination of high-porosity activated carbon obtained from dehydration of white sugar for electrochemical capacitor applications. ACS Sustainable Chemistry & Engineering, 7(1), 537-546.

[21] S. W. L. Ng, G. Yilmaz, W. L. Ong, G. W. Ho, Appl. Catal., B 2018, 220, 533.

[22] Ukkakimapan, P., Sattayarut, V., Wanchaem, T., Yordsri, V., Phonyiem, M., Ichikawa, S., ... & Endo, M. (2020). Preparation of activated carbon via acidic dehydration of durian husk for supercapacitor applications. Diamond and Related Materials, 107, 107906.

[23] Deshan, A. D. K., Forero, J. J., Bartley, J. P., Marasinghege, C., Tuiatua, K., Beltramini, J., & Doherty, W. O. (2021). Structural features of cotton gin trash derived carbon material as a catalyst for the dehydration of fructose to 5-hydroxymethylfurfural. Fuel, 306, 121670.

[24] Marsudi, M. A., Ma, Y., Prakoso, B., Hutani, J. J., Wibowo, A., Zong, Y., ... & Sumboja, A. (2020). Manganese oxide nanorods decorated table sugar derived carbon as efficient bifunctional catalyst in rechargeable Zn-air batteries. Catalysts, 10(1), 64.

[25] a) S.-E. Bae, K.-J. Kim, I.-H. Choi, S. Huh, Carbon 2016, 99, 8; b) Y. Kwon, K. Kim, H. Park, J. W. Shin, R. Ryoo, J. Phys. Chem. C 2018, 122, 4955.

[26] Chithra, A., Wilson, P., Vijayan, S., Rajeev, R., & Prabhakaran, K. (2021). Thermally insulating robust carbon composite foams with high EMI shielding from natural cotton. Journal of Materials Science & Technology, 94, 113-122.

[27] Matsagar, B. M., Yang, R. X., Dutta, S., Ok, Y. S., & Wu, K. C. W. (2021). Recent progress in the development of biomass-derived nitrogen-doped porous carbon. Journal of Materials Chemistry A, 9(7), 3703-3728.

[28] García-Bordejé, E., Pires, E., & Fraile, J. M. (2021). Carbon materials functionalized with sulfonic groups as acid catalysts. In Emerging Carbon Materials for Catalysis (pp. 255-298). Elsevier.

[29] Ishikawa, M., Egami, Y., & Shimizu, T. (2021). S-Encapsulated Micropore Carbon Cathode. Next Generation Batteries: Realization of High Energy Density Rechargeable Batteries, 357.

[30] L. Jiang, L. Sheng,Z. Fan, Sci. China Mater. 2018, 61, 133.

[31] Morgado, Sandra, et al. “Arbutus Unedo L.: From Traditional Medicine to Potential Uses in Modern Pharmacotherapy.” Journal of Ethnopharmacology, vol. 225, 2018, pp. 90–102, DOI:10.1016/j.jep.2018.07.004.

[32] Zou, X., Zhu, C., Wang, Q., & Yang, G. (2019). Catalytic dehydration of hexose sugars to 5-hydroxymethylfural. Biofuels, Bioproducts and Biorefining, 13(1), 153-173.

[33] Fernandes, F. A., Braga, T. R., Silva, E. O., & Rodrigues, S. (2019). Use of ultrasound for dehydration of mangoes (Mangifera indica L.): kinetic modeling of ultrasound-assisted osmotic dehydration and convective air-drying. Journal of food science and technology, 56(4), 1793-1800.

[34] Tran, T. T. V., Kongparakul, S., Karnjanakom, S., Reubroycharoen, P., Guan, G., Chanlek, N., & Samart, C. (2019). Highly productive xylose dehydration using a 16 sulfonic acid functionalized KIT-6 catalyst. Fuel, 236, 1156-1163.

[35] Jansrimanee, S., & Lertworasirikul, S. (2020). Synergetic effects of ultrasound and sodium alginate coating on mass transfer and qualities of osmotic dehydrated pumpkin. Ultrasonics Sonochemistry, 69, 105256.

[36] Aljammal, N., Jabbour, C., Thybaut, J. W., Demeestere, K., Verpoort, F., & Heynderickx, P. M. (2019). Metal-organic frameworks as catalysts for sugar conversion into platform chemicals: State-of- the-art and prospects. Coordination Chemistry Reviews, 401, 213064.

[37] Ciftyurek, E., Bragg, D., Oginni, O., Levelle, R., Singh, K., Sivanandan, L., & Sabolsky, E. M. (2019). Performance of activated carbons synthesized from fruit dehydration biowastes for supercapacitor applications. Environmental Progress & Sustainable Energy, 38(3), e13030.

[38] Lucas, N., Nagpure, A. S., Gurrala, L., Gogoi, P., & Chilukuri, S. (2020). Efficacy of clay catalysts for the dehydration of fructose to 5-hydroxymethyl furfural in biphasic medium. Journal of Porous Materials, 27(6), 1691-1700.

[39] Cháfer, M., Ortolá, M. D., Chiralt, A., & Fito, P. (2019). Orange peel products obtained by osmotic dehydration. In Osmotic Dehydration & Vacuum Impregnation (pp. 93-109). CRC Press.

[40] Nowacka, M., Dadan, M., & Tylewicz, U. (2021). Current applications of ultrasound in fruit and vegetables osmotic dehydration processes. Applied Sciences, 11(3), 1269.

[41] Perez, G. A. P., & Dumont, M. J. (2021). Polyvinyl sulfonated catalyst and the effect of sulfonic sites on the dehydration of carbohydrates. Chemical Engineering Journal, 419, 129573.

[42] Rezaie, M., Dinari, M., Chermahini, A. N., Saraji, M., & Shahvar, A. (2020). Preparation of kapa carrageenan-based acidic heterogeneous catalyst for conversion of sugars to high-value added materials. International Journal of Biological Macromolecules, 165, 1129-1138.

[43] Morawa Eblagon, K., Malaika, A., Ptaszynska, K., Pereira, M. F. R., & Figueiredo, J. L. (2020). Impact of Thermal Treatment of Nb2O5 on Its Performance in Glucose Dehydration to 5- Hydroxymethylfurfural in Water. Nanomaterials, 10(9), 1685.

[44] Poon, J. J., Tan, M. C., & Geow, C. H. (2020). Effects of Osmotic Dehydrated and Ultrasound Pre- Treated Orange Peel on Dye Removal. International Journal of Chemical and Process Engineering Research, 7(1), 1-11.

[45] Samilyk, M., Helikh, A., Bolgova, N., Potapov, V., & Sabadash, S. (2020). The application of osmotic dehydration in the technology of producing candied root vegetables. Eastern-European Journal of Enterprise Technologies, 3(11), 105.

[46] Kesavan, G., & Chen, S. M. (2020). Carbon-modified kaolin clay using sugar dehydration technique for the electrochemical detection of quercetin. Journal of Materials Science: Materials in Electronics, 31(23), 21670-21681.

[47] Estes, C. S., Gerard, A. Y., Godward, J. D., Hayes, S. B., Liles, S. H., Shelton, J. L., ... & Webster, H. F. (2019). Preparation of highly functionalized carbon nanoparticles using a one-step acid dehydration of glycerol. Carbon, 142, 547-557.

[48] Nicolae, S. A., Au, H., Modugno, P., Luo, H., Szego, A. E., Qiao, M., ... & Titirici, M. M. (2020). Recent advances in hydrothermal carbonisation: from tailored carbon materials and biochemicals to applications and bioenergy. Green Chemistry, 22(15), 4747-4800.

[49] Mahajan, A., & Gupta, P. (2020). Carbon-based solid acids: a review. Environmental Chemistry Letters, 18(2), 299-314.

[50] Fernández-Sanromán, Á., Lama, G., Pazos, M., Rosales, E., & Sanromán, M. Á. (2021). Bridging the gap to hydrochar production and its application into frameworks of bioenergy, environmental and biocatalysis areas. Bioresource Technology, 320, 124399.

[51] Kabbour, M., & Luque, R. (2020). Furfural as a platform chemical: From production to applications. Biomass, Biofuels, Biochemicals, 283-297.

[52] Cichowska, J., Figiel, A., Stasiak-Różańska, L., & Witrowa-Rajchert, D. (2019). Modeling of osmotic dehydration of apples in sugar alcohols and dihydroxyacetone (DHA) solutions. Foods, 8(1), 20.

[53] James, O. O., & Maity, S. (2022). Carbon-carbon (CC) bond forming reactions for the production of hydrocarbon biofuels from biomass-derived compounds. In Hydrocarbon Biorefinery (pp. 297-325). Elsevier.

[54] Sangregorio, A., Muralidhara, A., Guigo, N., Thygesen, L. G., Marlair, G., Angelici, C. Sbirrazzuoli, N. (2020). Humin based resin for wood modification and property improvement. Green Chemistry, 22(9), 2786-2798.

[55] Xu, L., Nie, R., Xu, H., Chen, X., Li, Y., & Lu, X. (2020). One-Pot Tandem Dehydration–Hydrogenation of Xylose with Formic Acid over Co Catalysts. Industrial & Engineering Chemistry Research, 59(7), 2754-2760.